THRESHOLDS FOR ELECTROPHYSIOLOGICAL IMPAIRMENT TO IN VIVO WHITE MATTER

Allison C. Bain and David F. Meaney
Department of Bioengineering
University of Pennsylvania

ABSTRACT

An in vivo, tissue-level, mechanical threshold for functional injury to CNS white matter was determined by comparing electrophysiological impairment to estimated tissue strain in an in vivo model of axonal injury. Axonal injury was produced by transiently stretching the right optic nerve of an adult male guinea pig to one of seven levels of ocular displacement (N_{level}=10; N_{total}=70). Functional injury was determined by the magnitude of the latency shift of the N_{35} peak of the visual evoked potentials (VEPs) recorded before and after stretch. A companion set of in situ experiments (N_{level}= 5) was used to determine the empirical relationship between ocular displacement and optic nerve stretch. Logistic regression analysis, combined with sensitivity and specificity measures and receiver operating characteristic (ROC) curves were then used to predict strain thresholds for axonal injury.

From this analysis, we determined three Lagrangian strain-based thresholds for electrophysiological impairment to the optic nerve tissue. The liberal threshold intended to minimize the false positive rate was a strain of 0.28, and the conservative threshold that minimized the false negative rate was 0.13. The optimal threshold criteria that balanced the specificity and sensitivity measures was 0.18. With this threshold data, it is now possible to predict more accurately the conditions that cause diffuse axonal injury in man.

THE MOST FREQUENT TYPE OF CLOSED HEAD INJURY, diffuse axonal injury (DAI), accounts for the second largest percentage of deaths due to brain trauma (Adams, Doyle et al. 1989). Although treatment paradigms are being developed for DAI, many areas of injury research now focus on developing the tools and techniques needed to prevent DAI. Central to understanding and evaluating preventive strategies for DAI is determining the local tolerance of the brain tissue to mechanical forces. Tissue tolerance data have become important as several finite element models emerge to transfer macroscopic head motions into estimates of the local stress and strain of the intracranial contents (Ruan, Khalil et al. 1991; Mendis 1992; Chu, Lin et al. 1993; Bandak and Eppinger 1994; Zhou, Khalil et al. 1994; Ueno, Melvin et al. 1995; Shreiber and Meaney 1998). Coupled together, validated finite element models and

tissue tolerance data offer a means to identify the hazardous mechanical environments that cause DAI, and offer a complete tool to design countermeasures for reducing the incidence and morbidity of this type of brain injury.

The goal of this investigation was to determine tissue-level thresholds for axonal injury using the guinea pig optic nerve stretch model (Gennarelli, Thibault et al. 1989). In this model, the loading conditions (i.e. tensile stretch) used to produce axonal injury are simple, and are easily controlled and quantified. Also, the simple architecture of the optic nerve permits straightforward quantification of the deformation of the tissue. Thus, it is easy to compare in vivo axonal injury to an experimentally measured strain value in order to define injury tolerances for the tissue.

In this study, we use the change in visual evoked potential caused by optic nerve stretch to determine a set of strain-based tissue-level thresholds that define the in vivo conditions associated with electrophysiological changes to the CNS white matter. In addition, we describe the ability of the proposed thresholds to predict morphological and functional axonal injury in practice, using measures of positive (PPV) and negative predictive value (NPV) (Einstein, Bodian et al. 1997; Shalev, Freedman et al. 1997; Varela, Bosco Lopez Saez et al. 1997).

METHODS

Optic Nerve Stretch Device - Briefly, the device delivers a reproducible, measurable amount of uniaxial displacement to the globe (0-10 mm) over a prescribed duration (60 ms) (Figure 1). A timing circuit controls the actuation of a linear solenoid (Lucas Ledex) used to produce the linear displacement. A linear variable differential transformer (LVDT) transducer (Trans-Tek Inc., Ellington, CT) and strain gauge force transducer (Entran, Fairfield, NJ) measure the magnitude of ocular displacement and the force experienced by the optic nerve, respectively. Both signals are recorded by a computer-based data acquisition system (Keithley-Metrabyte, Taunton, MA) sampling at a rate of 5 kHz.

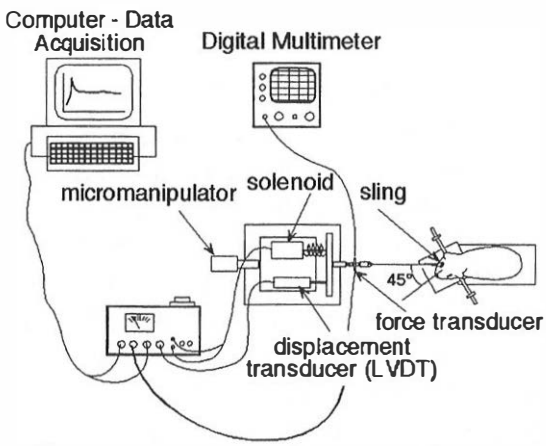

Figure 1 – Schematic overview of optic nerve stretch device

Although the optic nerve stretch device utilized in this investigation applies a known ocular displacement, the specific stretch transferred to the nerve is not explicit. Therefore, in situ experiments were first conducted to determine a quantitative relationship between applied ocular displacement and the resulting strain in the pre-chiasmatic region of the optic nerve.

Animal Preparation (in situ experiments) - Adult, male, albino, Hartley guinea pigs (600-700 grams) were euthanized with a lethal dose of sodium pentobarbital (60 mg/kg), and exsanguinated with 0.1% heparinized saline. After removing the skullcap and brain, the muscles and connective tissue surrounding the nerve were further dissected away to expose both optic nerves. One end of the guinea pig optic nerve is anatomically fixed to the base of the skull via a connective tissue bridge; this connection was left intact. The animal was placed on the stretch device in a manner identical to the in vivo experiments.

Using acrylic paint, small markers were placed at the endpoints of the optic nerve and evenly along its length (4 markers total). To examine fixation of the endpoint, a reference point was placed on the base of the skull. The nerve was preloaded (2 grams) and a photograph of the preloaded nerve was taken. The optic nerve stretch device was altered slightly to displace the globe at a strain rate of approximately 20 /sec, and hold it at maximum displacement until the trigger was released. A total of seven displacement levels were tested – 2, 3, 4, 5, 6, 7, and 8 mm. These levels encompassed the range of ocular displacements at which nerves were injured in the in vivo experiments. For each displacement level, five separate nerves were photographed at maximum displacement (N_{total} = 35).

Using the photographs of the preloaded nerve and the nerve at maximum displacement, the gauge length of the optic nerve and the displacement of each point with respect to the fixed endpoint were measured with digital calipers (Mitutoyo MTI Corp., Aurora, IL). For each group, the average nerve displacement was calculated and plotted versus ocular displacement. Linear regression analysis was used to calculate the approximated nerve displacement for each level of ocular displacement (Kaleidagraph, Synergy Software, Reading, PA). For each in vivo experiment, the approximated nerve displacement and the measured nerve gauge length were used to calculate the Lagrangian strain experienced by the optic nerve.

Animal preparation (in vivo experiments) – Animals were anesthetized with a mixture of ketamine (50 mg/ml) and xylazine (5 mg/ml). The right upper and lower eyelids were injected at the canthi with 2% lidocaine and were retracted with suture. Using iris scissors, a 360° opening was made in the conjunctiva and the six extraocular muscle insertions were severed. A sling constructed of sterile surgical material was placed around the posterior aspect of the globe so that the optic nerve projected out a slit in the sling. The animal was placed in the device stereotaxic head holder angled at 45° to align the optic nerve along the direction of displacement. The free ends of the sling were connected to the force transducer and the nerve was slightly preloaded (2 gms) immediately prior to stretch. The micromanipulator was adjusted to the prescribed magnitude of ocular displacement. Following stretch, the sling was cut free from the force transducer, the animal was removed from the stereotaxic head

holder, and the sling was removed from the globe. The animal was monitored until it was completely ambulatory and the as then returned to the animal facility. All surgical techniques were approved by the University of Pennsylvania's Institute for Animal Care and Use Committee (IACUC).

Electrophysiological Impairment - We quantified the functional impairment of the optic nerve by assessing changes in visual evoked potentials (VEPs) recorded before and after stretch. VEPs were measured in 30 of the 60 animals injured at six different levels of ocular displacement and in a set of sham animals ($N_{level} = 5$, $N_{total} = 35$).

Prior to surgery, two sterile needle electrodes were inserted under the scalp over the left and right visual cortex - 5 mm lateral to the midline and 2 mm anterior to the lamdoidal point. A third reference electrode was clipped to the left ear, and a ground electrode was attached to the right foot. The animal was placed in a grounded Faraday cage and was dark adapted for four minutes prior to each set of VEP measurements (Sokol 1976). After dark adaptation, a photostimulator presented unpatterned flashes from a lamp placed 20 cm from the right eye at a rate of 1.0 Hz (Grass Instruments, Astro-Med, Inc., West Warwick, RI). Each flash elicited the recording of the potential generated at the left visual cortex with respect to the reference electrode. Each signal was pre-amplified (1000x) and measured for 500 ms post-flash. VEPs were measured prior to surgery, every five minutes after stretch starting at eight minutes and ending at 48 minutes, and at sacrifice (72 hours).

All signals measured from the left visual cortex were digitally filtered with a Chebyshev 1-100 Hz bandpass filter (Matlab, Mathworks, Inc., Natick, MA). For each signal, the latency of the N_{35} peak was recorded. The latency shift of the N_{35} peak was calculated as the increase in latency from the pre-stretch level. Similar to the morphological injury analysis, we assigned a functional injury status to each nerve at every time point based on the magnitude of the measured latency shift. The mean and standard deviation of the latency of the N_{35} peak in VEPs measured from control animals were calculated and used to define presence or absence of functional injury. All latency shift recordings that fell outside two standard deviations of the average sham recording were labeled as injured (1); all other recordings were considered uninjured (0).

Logistic Regression Analysis - For each in vivo experiment, optic nerve strain was estimated using the predicted net displacement of the in situ optic nerve, and the measured gauge length of the pre-chiasmatic nerve measured at sacrifice. Morphological injury status and functional injury status at each recording time point were plotted versus this estimated optic nerve strain. Logistic regression analysis was performed to predict strain thresholds for morphological injury and for functional injury at the different time points (SYSTAT LOGIT Plug-in Module, SPSS, Inc. Chicago, IL). The logistic regression fit was considered significant for chi-squared values with $p<0.05$.

Threshold Analysis - For each logistic regression analysis, we calculated the sensitivity and specificity of the predicted strain values at 15 different probability levels (Altman 1991). In addition, a receiver operating characteristic (ROC) curve was constructed by plotting sensitivity versus 1-specificity for the different probability values. The area under each curve (AUC) was calculated and reported as a fraction of the maximum possible area. The AUC is a

normalized measure of the ability of optic nerve strain to discriminate between injured and uninjured nerves. A measure that predicts outcome 100% of the time has an AUC of 1.0; a measures that lacks discriminatory power, or predicts outcome no better than guessing, has an AUC of 0.50. In clinical practice, a good predictor generally achieves an AUC > 0.80 (Duke, Butt et al. 1997).

We used the receiver operator characteristics (ROC) curve analysis to define three potentially useful thresholds. First, we defined a "liberal" threshold (T_L) by the point on the ROC curve where the sensitivity attained its highest value at a specificity of 1.0. This threshold represents the point above which all nerves exhibit injury. Second, we defined a "conservative" threshold (T_C) by the point on the ROC curve where the specificity reached it highest value at a sensitivity equal to 1.0. Below this threshold, no nerves exhibit injury. Lastly, we defined an "optimal", or best, threshold (T_B), defined by the probability that maximizes the sum of the specificity and sensitivity (Fijten, Starmans et al. 1995).

Although sensitivity, specificity and ROC curves provide extensive information regarding the prognostic ability of a given test, they do not indicate the predictive ability of a threshold in a clinical situation (Altman 1991; Einstein, Bodian et al. 1997). Consequently, we evaluated the proposed thresholds based on their ability to predict injury by calculating positive predictive values (PPV) and negative predictive values (NPV) using information from the truth tables (Equations 1, 2) (Altman 1991).

$$PPV = \frac{TP}{TP + FP} \qquad [1]$$

$$NPV = \frac{TN}{TN + FN} \qquad [2]$$

Together, these measures provide an assessment of the efficacy of the chosen measure in practice. The closer PPV and NPV are to 1.0, the better the predictive measure is in practice. Ideally, a threshold should maximize both PPV and NPV.

RESULTS

In Situ Experiments - For each in situ experiment, we calculated the displacement of the nerve based on the change in distance between the nerve's marked endpoints. The anatomically fixed endpoint remained stationary for all experiments except those in the 8 mm stretch group. The slight movement of this fixed endpoint was accounted for in the nerve displacement measurements for these experiments. For each level of ocular displacement, we calculated the mean measured nerve displacement, the standard error, and the standard deviation (Table 1). The measured nerve displacements increased with increasing levels of ocular displacement, but were noticeably lower than the prescribed ocular displacements.

The mean gauge length (± standard deviation) measured for all nerves injured in the in vivo experiments was 8.40 ± 0.59 mm. When combined with the approximated nerve displacements, these gauge lengths corresponded to

nerve strains (E_{11}) between 0.10 and 0.50 for ocular displacements between 3-8mm.

OD (mm)	Mean ND	Standard Error	Standard Deviation	Approx. ND
2	0.70	0.053	0.092	0.59
3	1.02	0.032	0.071	1.00
4	1.23	0.020	0.046	1.41
5	1.78	0.048	0.107	1.81
6	2.29	0.094	0.210	2.22
7	2.56	0.105	0.235	2.63
8	3.11	0.093	0.207	3.03

Table 1: Mean nerve displacement (ND), standard error, standard deviation, and approximate nerve displacement were calculated for each level of ocular displacement (OD). Linear regression of the nerve displacement versus ocular displacement was used to calculate the approximated nerve displacement.

Electrophysiological Impairment - Pre-stretch VEPs were consistent among animals and between pre-stretch trials, and were very similar to those recorded by other investigators (Suzuki, Sitizyo et al. 1991; Suzuki, Sitizyo et al. 1991; Sima, Zhang et al. 1992; Takeuchi, Suzuki et al. 1992; Apaydin, Oguz et al. 1993). The mean latency (± standard deviation) of the N_{35} peak in pre-stretch recordings was 34.8 ms (± 1.1 ms). At all levels of ocular displacement, functional impairment of the optic nerve was noted at the earliest time point after stretch (8 minutes), as indicated by a latency shift of the N_{35} peak (Figure 2). Nerves injured at higher levels of ocular displacement generally showed greater degrees of N_{35} latency shift. In most cases, N_{35} latency gradually decreased after stretch, and returned to pre-stretch levels by 72 hours.

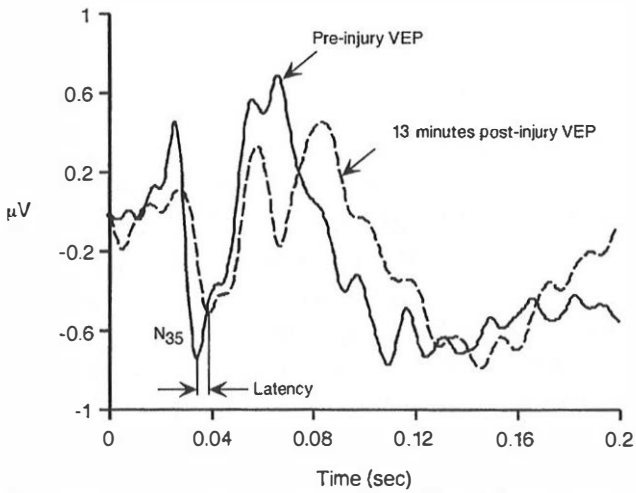

Figure 2 – Typical change in visual evoked potential. Changes in the latency of the N35 peak were used to measure the degree of impairment after stretch.

Logistic Regression Analysis - Logistic regression analysis of latency versus estimated tissue strain demonstrated high significance in estimating the model parameters (Likelihood Ratio Test, chi-squared, $p<0.0001$) at all time points except 72 hours. Also, McFadden's rho-squared values were very high for all time points up to 43 minutes (0.45-0.79). It was clear from this analysis that values predicted at 48 minutes and 72 hours lacked the statistical significance to predict thresholds for injury confidently; therefore, we only evaluated threshold values obtained by measurements up to 43 minutes post-stretch.

Threshold Analysis - For the eight time points being considered, the sensitivity and specificity for varying probabilities were used to construct eight separate ROC curves. The area under the ROC curve was greater than 0.94 at these time points, with the highest value occurring at 23 min. This indicated that latency shifts, measured from VEPs recorded up to 43 minutes after stretch, are very good indicators of functional impairment. Conservative threshold probabilities ranged from 10% at 18 and 23 minutes to 33% at 8, 13, 33, and 38 minutes. These probability values corresponded to strains between 0.09 and 0.18, with an average conservative threshold strain of 0.13. Similarly, liberal threshold probabilities ranged from 67% at 23 minutes to 99% at 33 and 38 minutes. These probabilities corresponded to strains between 0.18 and 0.47, with an average liberal threshold of 0.28.

By evaluating the plots of the sum of specificity and sensitivity, we found that the best probability threshold value varied among the different time points. The plot constructed at 8 minutes demonstrated that the 75% probability value maximized the sensitivity and specificity, whereas at 43 minutes, the 25% produced the largest sum (Figures 3a and 3b). However, strain values predicted at the different probability values were very similar among the time points (Table 2). For example, logistic regression analysis predicted a 75% tissue-level strain threshold of 0.17 at 8 minutes and a 25% strain threshold of 0.18 at 43 minutes. Thus, the best, overall threshold strain for in vivo functional impairment was 0.18 ± 0.01 (standard deviation).

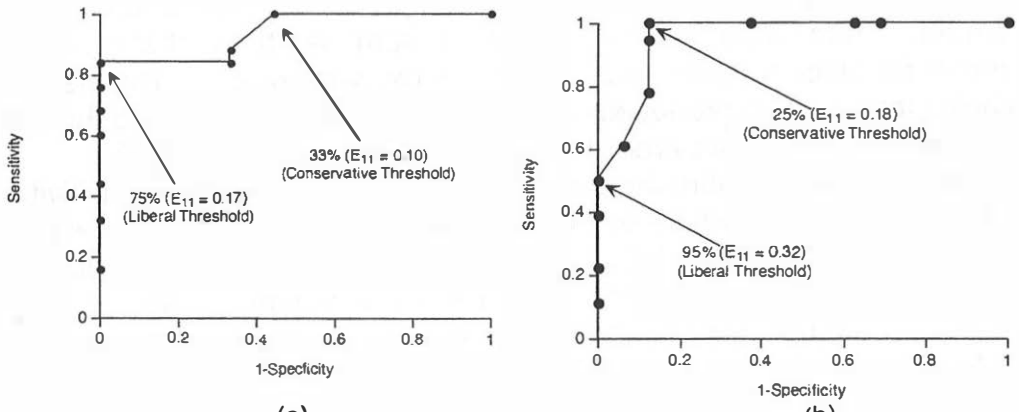

Figure 3 – Receiver operating characteristic curves for functional injury at (a) eight minutes post-stretch and (b) 43 minutes post-stretch.

The predictive values were calculated for all three thresholds for each time point. The conservative thresholds all had NPVs of 1.0. The PPVs for this threshold ranged from 0.79 at 28 minutes to 0.90 at 43 minutes, with an

average PPV of 0.85. The liberal thresholds achieved PPVs of 1.0 and a range of NPVs from 0.49 at 33 and 38 minutes to 0.92 at 23 minutes. The average NPV for the liberal thresholds was 0.67. The PPV and NPV calculated for the optimal threshold ranged from 0.69 to 1.00, with an average PPV of 0.94 and an average NPV of 0.88 (Table 2).

Time Point (minutes post-injury)	Probability Value	Threshold Strain	95% Confidence Limits	PPV	NPV
8	75%	0.171	0.118, 0.295	1.000	0.692
13	75%	0.171	0.118, 0.295	1.000	0.692
18	67%	0.180	0.134, 0.284	0.952	0.769
23	50%	0.171	0.136, 0.316	1.000	0.923
28	33%	0.192	0.112, 0.230	0.947	0.933
33	33%	0.181	0.065, 0.234	0.857	1.000
38	33%	0.181	0.065, 0.234	0.857	1.000
43	25%	0.182	0.071, 0.223	0.900	1.000

Table 2: The probability value that maximized the sum of the sensitivity and specificity of the functional injury data were reported for the eight different time points. At these different probability values we found the threshold strains predicted by the logistic regression to be very similar.

DISCUSSION

In this investigation, we combined information about the strains experienced in the guinea pig optic nerve with morphological and functional injury data to determine tissue-level thresholds for in vivo axonal injury. From logistic regression and ROC curve analyses, we found that the strain experienced by the optic nerve is a very good predictor of electrophysiological impairment. From these analyses, we also determined three strain-based thresholds for electrophysiological impairment in white matter. The first threshold strain of 0.28 produced a specificity of 1.00, and refers to the strain above which all nerves are predicted to exhibit changes in the VEP. Conversely, the second threshold prediction of 0.13 produced a sensitivity of 1.00 and defines the strain below which no nerves will show impairment. The final threshold criteria of 0.18 optimized both the specificity and sensitivity.

This investigation provides new information concerning in vivo, tissue-level thresholds for axonal injury based on experimentally measured strains. The ability to accomplish this task relied primarily on the uniqueness of the guinea pig optic nerve stretch model. Using this model, we were able to produce graded VEP impairments in vivo in a discrete, isolated segment of the CNS using very simple and controlled loading conditions. Furthermore, the accessibility of the optic nerve enabled us to visualize the deformation response of the nerve to varying levels of stretch, and thus quantify the strain experienced by the nerve during an experiment.

In the past, estimates for the tolerance of white matter tissue were derived from a combination of an experimental model with a physical or computational model to estimate the strains experienced by the tissue. For example, Mendis (Mendis 1992) matched oriented strain values determined from a finite element model of the primate brain to experimental injury, and found moderate DAI to occur at strains of 28%. Also, in a similar analysis, strains observed in a physical model of inertial injury were compared to injury in a primate brain to arrive at shear strain thresholds for moderate to severe DAI of 9.4% (Margulies and Thibault 1992). In both investigations, the limitations of the physical and computational models were recognized. Assumptions about the boundary conditions and the brain material properties and geometry affect the measured or predicted intracranial deformations. Validating the model's response with experimentally measured variables increases the reliability of strain approximations; however, it is very difficult and frequently impossible to make experimental measurements in many models of axonal injury.

By using the optic nerve model, we were able to alleviate concerns raised in previous investigations for determining white matter tolerances. We determined the strain experienced by the optic nerve from in situ experiments that were very similar to the in vivo condition. By measuring strain directly from the nerve, we did not have to estimate its material properties or approximate the behavior of the nerve. Also, we used the in situ experiments to show that the strain field in the optic nerve is primarily uniform within the range of displacements utilized in the in vivo experiments. Unlike many biological tissues, which often exhibit non-uniform strain patterns, the optic nerve has a very regular geometry with a cross-sectional area and microstructure that are relatively constant along the length of the nerve (Fine and Yanoff 1979). These characteristics are most likely responsible for the uniform strain patterns we observed in the in situ experiments. The uniformity obviated the need to compare specific strain patterns to complex injury patterns; thus, the location of detectable injury was unimportant toward the determination of an injury threshold. While a direct comparison of our thresholds with results obtained from physical and/or computational models may not be appropriate because of differences in the threshold variable (tensile vs. shear strain) and in the definition of injury (DAI vs. isolated axonal injury), it is worth noting that our determined thresholds for morphological injury fall within the range presented previously (Margulies and Thibault 1992; Mendis 1992).

In addition to developing thresholds for axonal injury, this investigation has expanded on this information by critically analyzing the chosen thresholds using measures of sensitivity, specificity, and predictive value, as well as ROC curves. These techniques have been used extensively in clinical research to assess the efficacy of different pharmacological drugs, treatments paradigms, and to evaluate the performance of diagnostic tests. The use of ROC curve analysis is offers two principal improvements over previous strategies to determine injury criteria. First, the area under the ROC curve, defined as a fraction of the maximum possible area (1.0), is a unique, numerical measure of the accuracy or performance of a test (Einstein, Bodian et al. 1997; Hajian-Tilaki, Hanley et al. 1997; Pastor, Menendez et al. 1997). The AUC is independent of the interpreted threshold, and therefore indicates the general

ability of the test variable to discriminate between a positive and negative outcome (Diamond 1992; Hajian-Tilaki, Hanley et al. 1997). Prior to choosing specific threshold values in the current analysis, the calculated AUC values for electrophysiology were very high. We concluded that the strain experienced by the optic nerve could be used effectively as an indicator of functional impairment. Interestingly, having a numerical measure of a variable's ability to indicate injury would also allow a direct comparison of different mechanical parameters. The second advantage to using ROC curves is that they provide information about the choice of a specific cut-off value or threshold for a set of data (Allaouchiche, Jaumain et al. 1996). Thresholds proposed in the engineering literature are frequently based on either the "average" response - the 50% value - or a much lower, more conservative value (Muckart, Bhagwanjee et al. 1997; Atkinson, Haut et al. 1998; Shreiber and Meaney 1998). Although these probability values are logical choices, they do not necessarily produce the best sensitivity, specificity, and predictive value as other probability values.

In closing, we believe the tissue-level thresholds determined herein to be a first step in developing thresholds for human axonal injury. These data can provide important insight into the local stress/strain conditions that are associated with traumatic axonal damage in vivo. When combined with more sophisticated finite element models that identify the relationship between head motions and brain tissue stress/strain response, one can predict more accurately the conditions (i.e. head rotational acceleration, rotational velocity, etc.) that cause diffuse axonal injury in man. In turn, the knowledge of the kinematic and/or kinetic conditions that cause diffuse axonal injury in man will lead to the development of effective countermeasures for reducing the incidence and severity of this brain injury victims of motor vehicle accidents.

REFERENCES

Adams, J. H., D. Doyle, I. Ford, T. A. Gennarelli and D. I. Graham (1989). "Diffuse axonal injury in head injury: Definition, diagnosis and grading." Histopathology **15**: 49-59.

Allaouchiche, B., H. Jaumain, C. Dumontet and J. Motin (1996). "Early diagnosis of ventilator-associated pneumonia: Is it possible to define a cutoff value of infected cells in BAL fluid." Chest **110**(6): 1558-1565.

Altman, D. (1991). Practical Statistics For Medical Research. New York, Chapman & Hall.

Apaydin, C., Y. Oguz, A. Agar, P. Yargicoglu, N. Demir and G. Aksu (1993). "Visual evoked potentials and optic nerve histopathology in normal and diabetic rats and effect of ginkgo biloba extract." Acta Opthalmologica **71**: 623-628.

Atkinson, T., R. Haut and N. Altiero (1998). "Impact-induced fissuring of articular cartilage: An investigation of failure criteria." Journal of Biomechanical Engineering **120**: 181-187.

Bandak, F. A. and R. H. Eppinger (1994). A three-dimensional finite element analysis of the human brain under combined rotational and translational accelerations. 38th Stapp Car Crash Conference, Ft. Lauderdale, FL, SAE.

Chu, C. S., M. S. Lin, H. M. Huang and M. C. Lee (1993). "Finite element analysis of cerebral contusion." Journal of Biomechanics **27**(2): 187-194.
Diamond, G. (1992). "Clinical epistemology of sensitivity and specificity." Journal of Clinical Epidemiology **45**(1): 9-13.
Duke, T., W. Butt and M. South (1997). "Predictors of mortality and multiple organ failure in children with sepsis." Intensive Care Medicine **23**: 684-692.
Einstein, A., C. Bodian and J. Gil (1997). "The relationships among performance measures in the selection of diagnostic tests." Archives of Pathology and Laboratory Medicine **121**: 110-117.
Fijten, G., R. Starmans, J. Muris, H. Schouten, G. Blijham and J. Knottnerus (1995). "Predictive value of signs and symptoms for colorectal cancer in patients with rectal bleeding in general practice." Family Practice **12**(3): 279-286.
Fine, B. and M. Yanoff (1979). Ocular Histology, Second Edition. New York, Harper & Row, Publishers.
Gennarelli, T. A., L. E. Thibault, R. Tipperman, G. Tomei, R. Sergot, M. Brown, W. L. Maxwell, D. I. Graham, J. H. Adams, A. Irvine, L. M. Gennarelli, A. C. Duhaime, R. Boock and J. Greenberg (1989). "Axonal injury in the optic nerve: A model simulating diffuse injury in the brain." Journal of Neurosurgery **71**: 244-253.
Hajian-Tilaki, K., J. Hanley, L. Joseph and J. Collet (1997). "A comparison of parametric and nonparametric approaches to ROC analysis of quantitative diagnostic tests." Medical Decision Making **17**: 94-102.
Margulies, S. S. and L. E. Thibault (1992). "A proposed tolerance criterion for diffuse axonal injury in man." Journal of Biomechanics **25**(8): 917-923.
Mendis, K. (1992). Finite element modeling of the brain to establish diffuse axonal injury criteria, Ohio State University.
Muckart, D., S. Bhagwanjee and E. Gouws (1997). "Validation of an outcome prediction model for critically ill trauma patients without head injury." The Journal of Trauma: Injury, Infection, and Critical Care **43**(6): 934-938.
Pastor, A., R. Menendez, M. Cremades, V. Pastor, R. Llopis and J. Aznar (1997). "Diagnostic value of SCC, CEA and CYFRA 21.1 in lung cancer: A Bayesian analysis." European Respiratory Journal **10**: 603-609.
Ruan, J. S., T. Khalil and A. I. King (1991). "Human head dynamic response to side impact by finite element modeling." Journal of Biomechanical Engineering **113**: 276-283.
Shalev, A., S. Freedman, T. Peri, D. Brandes and T. Sahar (1997). "Predicting PTSD in trauma survivors: Prospective evaluation of self-report and clinician-administered instruments." British Journal of Psychiatry **170**: 558-564.
Shreiber, D. I. and D. F. Meaney (1998). "Finite element analysis of traumatic brain injury in the rat." Journal of Biomechanical Engineering **(submitted)**.
Sima, A. A. F., W. X. Zhang, P. V. Cherian and S. Chakrabarti (1992). "Impaired visual evoked potential and primary axonopathy of the optic nerve in the diabetic BB/W-rat." Diabetologia **35**: 602-607.
Sokol, S. (1976). "Visually evoked potentials: Theory, techniques and clinical applications." Survey of Ophthalmology **21**(1): 18-44.

Suzuki, M., K. Sitizyo, T. Takeuchi and T. Saito (1991). "Changes in the visual evoked potentials with different photic conditions in guinea pigs." Journal of Veterinary Medicine and Science **53**(5): 911-915.
Suzuki, M., K. Sitizyo, T. Takeuchi and T. Saito (1991). "Visual evoked potential from scalp in guinea pigs." Journal of Veterinary Medicine and Science **53**(2): 301-305.
Takeuchi, T., M. Suzuki, K. Sitizyo, R. Isobe, T. Saito, T. Umemura and A. Shimada (1992). "Visual evoked potentials in guinea pigs with brain lesion." Journal of Veterinary Medicine and Science **54**(5): 813-820.
Ueno, K., J. W. Melvin, L. Li and J. W. Lighthall (1995). "Development of tissue level brain injury criteria by finite element analysis." Journal of Neurotrauma **12**(4): 695-706.
Varela, A., J. Bosco Lopez Saez and D. Quintela Senra (1997). "Serum ceruloplasmin as a diagnostic marker of cancer." Cancer Letters **121**: 139-145.
Zhou, C., T. B. Khalil and A. I. King (1994). Shear stress distribution in the porcine brain due to rotational impact. 38th Stapp Car Crash Conference Proceedings, Ft. Lauderdale, FL, SAE.